LOSSLESS CODING FOR PROGRESSIVE ARCHIVAL OF MULTISPECTRAL IMAGES

A. Benazza-Benyahia (1), *J-. C. Pesquet* (2), *M. Hamdi* (1)

(1) Dept. MASC, SUP'COM, Route de Raoued 3.5 Km, Cité El Ghazala, 2083 Ariana, Tunisia.
(2) Laboratoire Systèmes de Communication, Université de Marne-la-Vallée,
5, Bd Descartes, Champs sur Marne, 77454 Marne la Vallée Cédex 2, France.
E-mail: ben.yahia@planet.tn, pesquet@univ-mlv.fr

ABSTRACT

In this paper, a nonlinear subband decomposition scheme with perfect reconstruction is proposed for lossless coding of multispectral images. The merit of this new scheme is to exploit efficiently both the spatial and the spectral redundancies contained in a multispectral image sequence. Besides, it is suitable for progressive coding, which constitutes a desirable feature for telebrowsing applications. Simulation tests performed on real scenes allow to assess the performances of this new multiresolution coding algorithm. They demonstrate that the achieved compression ratios are higher than those obtained with currently used lossless coders.

1. INTRODUCTION

Multispectral images are of interest for a great number of applications such as target imaging, terrain mapping applications, meteorology,... Generally, these images are supplied by satellites observing the earth in several channels. For instance, the "Satellite Pour l'Observation de la Terre" (SPOT) has two High Resolution Visible imaging systems (HRV1 and HRV2). Each HRV is designed to operate in two modes of sensing: a 10 m resolution "Panchromatic" (P) mode over the range [0.5-0.73] μm and a 20 m resolution multispectral mode. For the multispectral mode, the XS1 channel is associated with the range [0.5-0.59] μm, the XS2 channel with the range [0.61-0.78] μm and the XS3 band with the range [0.79-0.89] μm. Therefore, for the same scene, the 4 bands P, XS1, XS2, XS3 and XS4 are available.

Larger and larger amounts of data are generated thanks to the continuous improvement and increased popularity of remote sensing systems. The problem of managing, transmitting and archiving such a tremendous volume of data is crucious. To give an idea of the importance of the problem, recall that a scene acquired by the Thematic Mapper sensors corresponds to about 200 Mbytes. This amount of data requires huge storage capabilities as well as a large transmission bandwidth during downlinking. Therefore, it is really challenging to develop image compression techniques so as to provide solutions to this problem. Two types of schemes can be envisaged: lossy or lossless. In this paper, we focus our attention on lossless coding techniques for multispectral remotely sensed images because we are mainly interested in archiving applications. Indeed, archival storage of images requires exact reproducibility of the data since the least distortion may lead to an erroneous interpretation of the considered scene or to the computation of incorrect ground parameters. Therefore, it must be possible to perfectly recover the original image. Furthermore, progressive reconstruction is a desirable feature for telebrowsing through images databases. It consists in encoding the image in several layers: the first level corresponds to a very highly compressed version and each successive level provides more details until ultimately the image is completely recovered. Such gradual reconstruction requires a compact and non-redundant pyramidal representation of the input image. Nonlinear subband decompositions have been developped recently [1, 2, 3]. They provide hierarchical and compact representations for gradual coding of images [4] and, for this reason, they have been retained in the standard JPEG 2000 [5]. To the best of our knowledge, the problem of extending such kind of representations to multispectral images has not yet been addressed. Indeed, in existing methods, each spectral component is very often coded independently of the others. In this paper, we develop a new algorithm which exploits the mutual dependences between spectral bands thanks to generalized nonlinear subband decompositions. This paper is organized as follows. In Section 2, we briefly describe the related works in the field of lossless coding of multispectral images so as to better define our contribution. In Section 3, we propose a new hybrid hierarchical and reversible decomposition which exploits both the spectral and the spatial redundancies. Finally, in Section 4, we provide some experimental results and compare them to the performances of conventional methods.

2. A SHORT REVIEW OF EXISTING LOSSLESS CODERS

Usually, differential predictive coders are applied to compress multispectral data [6]. More precisely, let $\{s^{(b)}(m,n)\}_{b=1,\dots,B}$ be a 2D multiband where B is the number of spectral bands and let $\hat{s}^{(b)}(m,n)$ denote the predicted value of the current pixel $s^{(b)}(m,n)$. Among the spatial coders, the Optimal Linear Predictor (OLP) based on the 3 nearest previous neighbors can be easily applied. The prediction coefficients are solutions of the normal equations. It is also possible to use predetermined coefficients for the predictors as in the JPEG standard [7]. The user retains the best one in terms of entropy (BJPEG). The Context-based Adaptive Lossless Image Codec (CALIC) is another nonlinear predictor [8]. A gradient-adjusted predictor is applied: the prediction is a linear combination of the surrounding pixels according to the estimated gradient. Recently, the Consultative Committee for Space Data Systems (CCSDS) has adopted a standard for lossless data compression, based on extended version of Rice algorithm [9]. The CCSDS standard consists of a prediction followed by Rice entropy encoding. Initially, the applied predictor is a 1D nearest-neighbor predictor. An effort has been made in order to propose other predictors (spatial, spectral or hybrid) [10]. Therefore, the predictor which yields the best compression ratio is selected. Spectral coders take into account the spectral redundancies by using only the pixels of the remaining bands. In [11], a simple Monoresolution Spectral Coding (MSC) was proposed for SPOT images ($B = 3$). It consists in coding the band $s^{(b_0)}(m,n)$ with an OLP in a purely spatial mode. Then, the remaining images $s^{(b_1)}(m,n)$ and $s^{(b_2)}(m,n)$) are predicted according to:

$$\left\{ \begin{array}{lcl} \hat{s}^{(b_1)}(m,n) & = & p_0 s^{(b_0)}(m,n) \\ \hat{s}^{(b_2)}(m,n) & = & p_1 s^{(b_0)}(m,n) + p_2 s^{(b_1)}(m,n) \end{array} \right. , \quad (1)$$

where the coefficients p_0, p_1, p_2 are solutions of normal equations. We will denote MSC(b_0, b_1, b_2) the decomposition starting by b_0, followed by b_1 and then by b_2.

Generally, it is more appropriate to capture simultaneously the spectral and the spatial correlations by applying hybrid predictors. For SPOT images, it is proposed in [11] to predict the multiband signal component by component. The first band b_0 is predicted by using the previous samples for all the bands. The prediction of the second band includes additionally $s^{(b_0)}(m,n)$. Finally, both $s^{(b_0)}(m,n)$ and $s^{(b_1)}(m,n)$ are incorporated in the prediction of the last band b_2. The coefficients achieving the minimum error variance are solutions of 3 linear systems. More recently, an interband version of CALIC based on a gradient adjusted interband predictor was proposed [12]. A switching procedure betweeen the two modes (purely spatial/purely spectral) is described. Again, it is possible to use fixed predictors as proposed in [10]. Finally, in a recent paper [13], a lossless compression of multispectral images based on 3D fuzzy prediction was proposed.

However, in the context of lossless *and* progressive coding of multispectral images, there are few publications. Recently, in [11], the problem of lossless *and* hierarchical coding of SPOT images was addressed and a hybrid *two-step* method was investigated. Firstly, the bands are spatially decorrelated by means of a reversible intraband wavelet transform [2]. More precisely, a lifting scheme of depth J is applied separately on each band. Then, the spectral correlations existing between the $3J+1$ resulting bands are exploited by the MSC purely spectral coder. The contribution consists in using MSC acting on each triplets of subbands which have the same resolution level and the same orientation.

In the next section, we will describe a new method of exact and gradual coding of multispectral images.

3. PROPOSED INTERBAND DECOMPOSITION

3.1. Multiresolution intraband decompositions

First of all, let us describe the nonlinear intraband decomposition tools which are the origin of our work. Figure 1 shows a class of nonlinear M-band decomposition schemes proposed in [3]. The resulting subbands can be obtained by the following equations:

$$\begin{array}{ll} y_1 & = \mathcal{A}_1[x_1] + \mathcal{C}_1[z_2, \ldots, z_M] \\ y_i & = \mathcal{A}_i[x_i] + \mathcal{B}_i[\mathcal{A}_1[x_1], \ldots, \mathcal{A}_{i-1}[x_{i-1}]] + \\ & \mathcal{C}_i[z_{i+1}, \ldots, z_M] \quad (i = 2, \ldots, M-1) \\ y_M & = \mathcal{A}_M[x_M] + \mathcal{B}_M[\mathcal{A}_1[x_1], \ldots, \mathcal{A}_{M-1}[x_{M-1}]] \end{array} \quad (2)$$

where $x_1, \ldots, x_M$ are the M-polyphase components of the 1D signal x to be coded. Furthermore, we have:

$$\forall i \in \{2, \ldots, M-1\},\ z_i = y_i - \mathcal{C}_i[z_{i+1}, \ldots, z_M], \quad z_M = y_M. \quad (3)$$

Exact reconstruction holds for any operators $\mathcal{B}_i$, $\mathcal{C}_i$ and injective operators $\mathcal{A}_i$ for $i \in \{1, \ldots, M\}$ [3]. Such subband decomposition with perfect reconstruction is a very versatile tool for building multiresolution decompositions. The $\mathcal{B}_i$'s decorrelate the input signals and the $\mathcal{C}_i$'s smooth the associated input. Extension to 2D signal is handled in a separable manner. The decomposition structure has the merit to provide a unifiying framework for lossless compression schemes based on nonlinear multiresolution analyses [14]. Indeed, the concept of lifting developed by Sweldens *et al.* [2] corresponds to a structure which is included in this scheme with $M = 2$. Several examples of such operators have been already tabulated in [2]. In the following, $c_{N,\tilde{N}}$ denotes the wavelet transforms with N (resp. $\tilde{N}$) vanishing moments of the analyzing (resp. synthesizing) high-pass filters. The S+P transform is another compelling transform proposed by Said and Pearlman [1].

3.2. The proposed extension

The objective of this paper consists in adapting the decomposition in Fig. 1 to the case of a multispectral signal in order to exploit *both* the spatial and spectral correlations. The multispectral case is actually similar to an $M = 2B$ band decomposition. In the intraband decomposition described previously, the input signal are polyphase components of a *single* band approximation at the current resolution level j. Now, the even and the odd samples of *several* approximation bands $s_j^{(1)}(2n), \ldots, s_j^{(B)}(2n), s_j^{(1)}(2n+1), \ldots, s_j^{(B)}(2n+1)$ constitute the $2B$ input coefficients:

$$\forall b \in \{1, \ldots, B\},\ x_b(n) \triangleq s_j^{(b)}(2n), \quad x_{b+B}(n) \triangleq s_j^{(b)}(2n+1). \quad (4)$$

The operators $\mathcal{B}_1, \ldots, \mathcal{B}_{2B}$ and $\mathcal{C}_1, \ldots, \mathcal{C}_{2B}$ are hybrid (intraband and interband) prediction and updating operators. The $2B$ outputs can be classified into 2 classes: the prediction errors $d_{j+1}^{(1)}, \ldots, d_{j+1}^{(B)}$ and the approximation coefficients $s_{j+1}^{(1)}, \ldots, s_{j+1}^{(B)}$:

$$\forall b \in \{1, \ldots, B\},\ y_b(n) \triangleq s_{j+1}^{(b)}(n), \quad y_{b+B}(n) \triangleq d_{j+1}^{(b)}(n). \quad (5)$$

Although the dependences existing between the bands could be extracted by a wide class of nonlinear operators, they are more easily handled by linear filters followed by rounding operations. In a previous work, we have already considered a very simplified case of such a decomposition involving linear predictors [15]. For a given band b_0, a general expression of the prediction error at resolution $(j+1)$ is given by:

$$d_{j+1}^{(b_0)}(n) = s_j^{(b_0)}(2n+1) - \lfloor \sum_{b=1}^{B} \sum_{l \in \mathcal{P}_{j,b_0}^{(b)}} p_{j,b_0,l}^{(b)} s_j^{(b)}(2n-l) \rceil, \quad (6)$$

where the set $\mathcal{P}_{j,b_0}^{(b)}$ is the support of the predictor of band b_0 from band b at stage j. The coefficients $p_{j,b_0,l}^{(b)}$ are the weights of this predictor. Similarly, it is possible to express the approximations as follows:

$$\begin{aligned} s_{j+1}^{(b_0)}(n) = s_j^{(b_0)}(2n) + \lfloor \sum_{b=1}^{B} \sum_{l \in \mathcal{U}_{j,b_0}^{(b)}} u_{j,b_0,l}^{(b)} d_{j+1}^{(b)}(n-l) \\ + \sum_{b=1}^{B} \sum_{l \in \mathcal{U'}_{j,b_0}^{(b)}} {u'}_{j,b_0,l}^{(b)} s_j^{(b)}(2n-l) \rceil. \end{aligned} \quad (7)$$

Finally, the case of a 2D multiband signal (multispectral images) is handled by means of a separable decomposition.

3.3. Conditions for exact recovery

For an exact recovery, it is necessary that at least for one band (say b_0), all the sets $\mathcal{U}'^{(b)}_{j,b_0}$ are empty *i.e.* only detail coefficients are involved in the computations of $s^{(b_0)}_{j+1}(n)$. For the remaining bands b_i, $i \in \{1,2\}$, the sets $\mathcal{U}'^{(b)}_{j,b_i}$ must contain only even indices. Indeed, the first reconstruction step consists in calculating the even samples $s^{(b_0)}_j(2n)$ from $s^{(b_0)}_{j+1}(n)$ and $d^{(b_0)}_{j+1}(n)$ by "reversing" Eq. (7). Then, it is possible to recover the other even samples $s^{(b_i)}_j(2n)$ in the same way.

To recover the odd samples $s^{(b_0)}_j(2n+1)$, some care must be taken about the used neighborhoods and the order of decomposition of the bands. Indeed, to compute the prediction term of a band b_0 from a band b, the samples $s^{(b)}_j(2n-l)$ for $l \in \mathcal{P}^{(b_0)}_{j,b}$ must be avalaible. Consequently, only the following situations are allowed:

- For a couple of indices (b, b_0) $(b \neq b_0)$, if both $\mathcal{P}^{(b)}_{j,b_0}$ and $\mathcal{P}^{(b)}_{j,b_0}$ contain only even samples, the bands b and b_0 can be decomposed in any order and it is possible to calculate the contribution of band b to the prediction of band b_0.
- Let us now consider the case where the set $\mathcal{P}^{(b)}_{j,b_0}$ contains some odd indices. For the sake of clarity, suppose that $\mathcal{P}^{(b)}_{j,b_0}$ contains odd indices $l_1, \ldots, l_K$. The samples $s^{(b)}_j(2n-l_1), \ldots, s^{(b)}_j(2n-l_K)$ must be avalaible in order to reconstruct the contribution of band b to the prediction of band b_0. A straightforward solution consists in constraining the $\mathcal{P}^{(b_0)}_{j,b}$ to contain only even indices. Thus, it would be possible to recover firstly the approximation $s^{(b)}_j(n)$ (in particular, the odd samples of band b) before proceeding to the reconstruction of band b_0.
- The support $\mathcal{P}^{(b_0)}_{j,b_0}$ must contain either positive odd indices (past samples and causal processing) or negative odd indices (future samples and anticausal processing).

3.4. Retained solution

In our simulations, we have extended in different ways the usual decompositions $c_{N,\tilde{N}}$. For the sake of clarity, we present here a generalization of the $c_{2,2}$ decomposition. The b_0 image is predicted according to:

$$d^{(b_0)}_{j+1}(n) = s^{(b_0)}_j(2n) - \lfloor \mathbf{p}_0^T \mathbf{s}^{(b_0)}_j(n) \rceil, \tag{8}$$

$$\text{where } \mathbf{s}^{(b_0)}_j(n) \triangleq \begin{pmatrix} s^{(b_0)}_j(2n-1) \\ s^{(b_0)}_j(2n+1) \\ s^{(b_1)}_j(2n-1) + s^{(b_1)}_j(2n+1) \end{pmatrix}. \tag{9}$$

The prediction of the b_1 image can be written as:

$$d^{(b_1)}_{j+1}(n) = s^{(b_1)}_j(2n) - \lfloor \mathbf{p}_1^T \mathbf{s}^{(b_1)}_j(n) \rceil, \tag{10}$$

$$\text{where } \mathbf{s}^{(b_1)}_j(n) \triangleq \begin{pmatrix} s^{(b_1)}_j(2n-1) \\ s^{(b_1)}_j(2n+1) \\ s^{(b_0)}_j(2n) \\ s^{(b_0)}_j(2n-1) \\ s^{(b_0)}_j(2n+1) \end{pmatrix}. \tag{11}$$

The b_2 image is predicted according to the following equation:

$$d^{(b_2)}_{j+1}(n) = s^{(b_2)}_j(2n) - \lfloor \mathbf{p}_2^T \mathbf{s}^{(b_2)}_j(n) \rceil, \tag{12}$$

$$\text{where } \mathbf{s}^{(b_2)}_j(n) \triangleq \begin{pmatrix} s^{(b_2)}_j(2n-1) \\ s^{(b_2)}_j(2n+1) \\ s^{(b_0)}_j(2n) + s^{(b_1)}_j(2n) \\ s^{(b_0)}_j(2n-1) + s^{(b_1)}_j(2n-1) \\ s^{(b_0)}_j(2n+1) + s^{(b_1)}_j(2n+1) \end{pmatrix}. \tag{13}$$

For b_1 and b_2, the update operations are similar:

$$\begin{cases} s^{(b_1)}_{j+1}(n) = s^{(b_1)}_j(2n-1) - \lfloor u_1(d^{(b_1)}_{j+1}(n-1) + d^{(b_1)}_{j+1}(n)) \rceil \\ s^{(b_2)}_{j+1}(n) = s^{(b_2)}_j(2n-1) - \lfloor u_2(d^{(b_2)}_{j+1}(n-1) + d^{(b_2)}_{j+1}(n)) \rceil \end{cases} \tag{14}$$

However, the update of b_0 includes the sample $s^{(b_1)}_j(2n-1)$:

$$\begin{aligned} s^{(b_0)}_{j+1}(n) = s^{(b_0)}_j(2n-1) - \lfloor & u_{0,1}(d^{(b_0)}_{j+1}(n-1) + d^{(b_0)}_{j+1}(n)) \\ & + u_{0,2}\, s^{(b_1)}_j(2n-1) \rceil. \end{aligned} \tag{15}$$

It is worth pointing out that the considered decomposition is perfectly reversible. Indeed, the odd samples $s^{(b_1)}_j(2n-1)$ and $s^{(b_2)}_j(2n-1)$ are easily recovered by reversing Eq. (14). Then, $s^{(b_0)}_j(2n-1)$ is directly obtained from Eq. (15). The even samples are recursively obtained starting with $s^{(b_0)}_j(2n)$ using Eq. (8), then with $s^{(b_1)}_j(2n)$ using Eq. (10) and finally with $s^{(b_2)}_j(2n)$ using Eq. (12).

3.5. Optimizing the operators

Obviously, the performances of the proposed decomposition in terms of compression are closely related to the choice of the predictors. The effectiveness of the lossless coding is measured by the zero-th order entropies $H = \sum_{b=1}^{B} H_b$ where H_b is the global entropy associated with the band b. For a J level decomposition, it is the weighted sum of the entropies of the approximation and detail sub-images. Our aim is to apply predictors ensuring a (local) minimum of H. Since the entropies are implicit functions of the parameters of the decomposition, a Nelder-Mead simplex algorithm is applied.

4. EXPERIMENTAL RESULTS

The simulation results are provided for a SPOT4 image depicting the city of Tunis (Tunisia). The correlation coefficient between XSk and XSl is denoted by ρ_{kl}. Since $\rho_{12} = 0.99$, $\rho_{13} = 0.65$ and $\rho_{23} = 0.64$, we deduce that XS1 is highly correlated with XS2. Therefore, it seems useful to exploit the mutual correlation between these two bands. Table 1 provides performances of some conventional lossless coders. We have retained only the best order of decomposition, mentioned by the triplet (b_0, b_1, b_2). The line "$c_{2,2}$ then MSC" corresponds to the two-stage hybrid procedure described in [11]: the $c_{2,2}$ transform decorrelates spatially the bands and the MSC decorrelates spectrally the images. Obviously, multiresolution representations are the most compact if we except the monoresolution coders ID#84 and ID#87 which do not allow progressive coding.

Since the bands XS1 and XS2 are highly correlated, it is appropriate to take either $(b_0, b_1, b_2) = (1, 2, 3)$ or $(b_0, b_1, b_2) = (2, 1, 3)$. Table 1 indicates that our method outperforms the existing coders and is even better than the competitive two-stage hybrid procedure. It also demonstrates that introducing a term from b_1 in the update of b_0 yields to decreased values for the entropy H.

5. REFERENCES

[1] A. Said, W.A. Pearlman, "An image multiresolution representation for lossless and lossy compression," *IEEE Trans. on IP*, vol. 5, pp. 1303-1310, September 1996.

[2] A.R. Calderbank, I. Daubechies, W. Sweldens, B.-L. Yeo, "Wavelet transforms that map integers to integers," *Appl. and Comput. Harmonic Analysis*, vol. 5, pp. 332-369, 1998.

[3] F. Hampson, J.C. Pesquet, "M-band nonlinear subband decompositions with perfect reconstruction," *IEEE Trans. on IP*, vol. 7, pp. 1547-1560, November 1998.

[4] M.D. Adams, F. Kossentini, "Reversible integer-to-integer wavelet transforms for image compression: performance evaluation and analysis", *IEEE Trans. on IP*, vol. 9, no. 6, pp. 1010-1024, June 2000.

[5] D. Santa-Cruz, T. Ebrahimi, "A study of JPEG2000 still image coding versus other standards," *Proc. of the X EUSIPCO*, Tampere, Finland, September 5-8, 2000.

[6] J. C. Tilton, D. Han, M. Manohar, "Compression experiments with AVHRR data," *Proc. of DCC*, pp. 411-420, 1991.

[7] JPEG, ISO/IEC 10918-1: Information technology- digital compression and coding of continuous-tone still images: requirements and guidelines, (1994).

[8] X. Wu, N.D. Memon, "Context-based adaptive lossless image coding," *IEEE Trans. on Commun.*, vol. 45, pp. 437-444, April 1997.

[9] *Lossless Data Compression*, CCSDS Recommendation for Space Data Systems Standards, Blue Book 120.0-B-1, Washington, D.C., May 1997.

[10] S.E. Qian, A.B. Hollinger, Y. Hamiaux, "Study of real-time data compression for hyperspectral imagery," *Proc. of the IEEE IGARSS*, Frankfurt, Germany, July 1999.

[11] G. Mozelle, "Compression de données multiples et dynamiques," Thèse de Doctorat, Univ. Paris V, France, 1998.

[12] X. Wu, N.D. Memon, "Context-based interband compression-extending CALIC," *IEEE Trans. on IP*, vol. 9, no. 6, pp.994-1001, June 2000

[13] B. Aiazzi, P. Alba, L. Alparone, S. Baronti, "Lossless compression of multi/hyper-spectral imagery based on a 3-D fuzzy prediction," *IEEE Trans. on GRS*, vol. 37, no. 5, pp. 2287-2289, September 1999.

[14] A. Benazza-Benyahia, J-. C. Pesquet, "A unifying framework for lossless and progressive image coding," *Proc. of the ISIVC*, Morocco, pp. 333-341, April 2000.

[15] A. Benazza-Benyahia, Z. Belhadj, J-.C. Pesquet, M. Hamdi, " Reversible and progressive coding of multispectral SPOT images," *Proc. of the IEEE IGARSS*, Honolulu, Hawai, USA, July 2000.

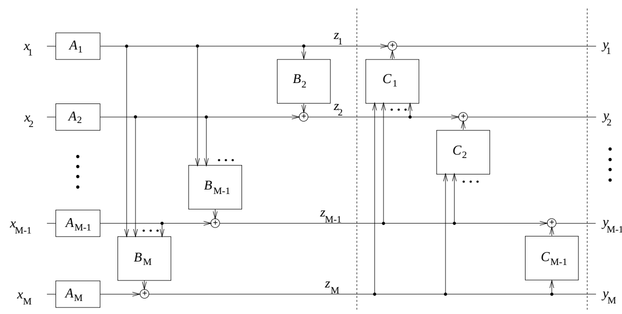

Fig. 1. Nonlinear M-band decomposition structure.

Table 1. Resulting entropies of lossless coders. The multiresolution decompositions have $J = 4$ stages.

Decomposition	H_1	H_2	H_3	H
Original	7.1988	7.3019	6.7289	21.2296
BJPEG	5.2203	5.3882	4.8366	15.4451
OLP	5.1311	5.2976	4.7382	15.1669
MSC (1,3,2)	5.1311	6.3316	6.7289	18.1916
ID#3 (1,2,3)	5.1311	4.9645	7.1417	17.2373
ID#84 (1,2,3)	5.1311	3.5700	5.7374	14.4385
ID#87 (1,2,3)	5.1311	3.6139	5.8040	14.5490
ID#100 (1,2,3)	5.1311	5.1311	6.1852	16.4474
ID#103 (2,1,3)	5.4979	5.2976	6.3832	17.1787
S+P	5.0184	5.1817	4.5971	14.7972
$c_{2,2}$	5.0748	5.2400	4.6639	14.9787
$c_{2,2}$ then MSC(1,3,2)	4.9664	4.6639	4.2158	13.8461
Proposed dec. (1,2,3) $u_{0,2} = 0$	5.0748	4.5295	4.6529	14.2634
Optimized parameters	5.0460	4.1317	4.6581	13.8407
Proposed dec. (2,1,3) $u_{0,2} = 0$	4.0015	5.2400	4.6596	13.9010
Optimized parameters	3.9842	5.0962	4.6555	**13.7359**